Journal of Applied Polymer Science

Anhydrous Proton-Conducting Electrolyte Based on a Nematic Poly(methyl acrylate) Containing Sulfonated Side Chains

Ting Liang, Yong Wu, Shuai Tan, Caihong Wang
Department of Process Equipment, College of Chemical Engineering, Sichuan University, Chengdu 610065, China
Correspondence to: Y. Wu (E-mail: wuyong@scu.edu.cn)

ABSTRACT: A nematic poly(methyl acrylate) containing terminal sulfonic acids in side chains was prepared by etherification of a brominated mesomorphic precursor with 2-hydroxyethanesulfonic acid sodium salt. Differential scanning calorimetry measurements and polarized light microscopy observation revealed that the sulfonated polymer exhibited the nematic mesophase at medium temperatures (189–227°C). Electrochemical impedance spectroscopy measurements showed that temperature dependence of anhydrous proton conductivity for the nematic polymer followed the Arrhenius law and that the estimated activation energy was 95 kJ mol^{-1} in the nematic phase. The proton conductivities of the nematic polymer were two orders of magnitude higher than those of anhydrous Nafion®117 membrane at the same temperature. The enhanced anhydrous proton conductivities of the polymeric electrolyte were ascribed to the orientational order and fluidity of the nematic liquid crystal. © 2014 Wiley Periodicals, Inc. J. Appl. Polym. Sci. **2014**, *131*, 40382.

KEYWORDS: liquid crystals; electrochemistry; conducting polymers

Received 9 October 2013; accepted 1 January 2014
DOI: 10.1002/app.40382

INTRODUCTION

Proton conduction plays a key role in various electrochemical devices such as fuel cells, batteries, chemical sensors, and displays.[1] Great success has been achieved with humidified perfluorosulfonic acid polymers (e.g., Nafion®117 membrane) acting as proton-conducting electrolytes for fuel cells.[2] Proton conduction in these highly hydrated polymers base majorly on transportation of hydronium ions through the vehicle mechanisms.[3,4] As a result, the operating temperature of fuel cells using the perfluorosulfonic acid polymers is limited to 100°C. However, higher operating temperatures have the advantages of enhancing electrode reaction rate and improving carbon monoxide tolerance in electrolyte membrane fuel cells.[5,6] In recent years, anhydrous proton-conductive polymers working at intermediate temperatures have attracted much interest from electrochemical technologies.[7–13]

Liquid crystals represent a class of unique soft matter materials combining anisotropy with dynamic nature.[14] Introduction of protongenic moieties into liquid crystals provides an alternative strategy to transport protons through the Grotthuss mechanism. Huang et al.[15] and Ueda et al.[16] prepared columnar liquid crystals by integrating sulfonic moieties with mesogenic fan-shaped molecules. The resultant sulfonic liquid crystals exhibited one-dimensional proton conduction after macroscopically aligned. Chow et al.[17] synthesized a smectic phenylsulfonic acid for transporting protons anhydrously. Recently, we exemplified that anhydrous proton conduction in the smectic sulfonated polymer could be enhanced by means of mechanical shearing.[18] All the mentioned works indicated that the positional order of sulfonated liquid crystals promoted proton conduction significantly by virtue of forming continuous proton-conducting pathways. Although a few smectic proton conductors have been well characterized, anhydrous proton conduction resulted from nematic electrolytes remains unexplored. Nematic is the simplest liquid crystal phase in which randomly positioned molecules arrange in a common preferred direction. The aim of this study is to investigate the effect of the nematic liquid crystal on anhydrous proton conduction in a polymeric electrolyte.

We prepared poly(methyl acrylate)-containing sulfonated side chains by etherification of a brominated mesomorphic precursor with 2-hydroxyethanesulfonic acid sodium salt. The resultant polymer was confirmed through the Fourier transform infrared (FTIR) and elemental analyses. The nematic phase at intermediate temperatures was identified by differential scanning calorimetry (DSC) and polarizing optical microscope (POM) observation. Electrochemical impedance spectroscopy (EIS) measurements revealed that temperature dependence of anhydrous proton conductivity for the polymeric electrolyte followed the Arrhenius law in the mesophase. At the same temperature, proton conductivities of the nematic electrolyte were two orders of magnitude higher than those of anhydrous Nafion®117 membrane. The nematic sulfonated polymer had

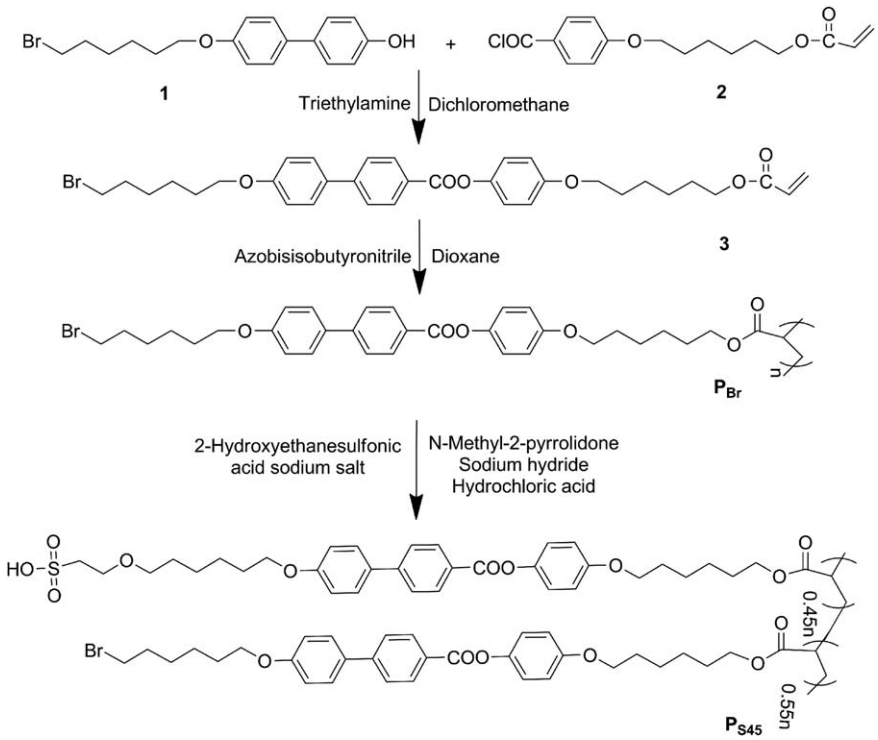

Scheme 1. Synthesis route of the sulfonated poly(methyl acrylate).

great potential in developing anhydrous electrolyte for fuel cells working at intermediate temperatures.

EXPERIMENTAL

The mesogenic polymer consists of poly(methyl acrylate) backbones and biphenyl benzoate-based side chains. Terminal sulfonic acid moieties were incorporated into the side chains by postpolymerization functionalization of a brominated mesomorphic precursor with 2-hydroxyethanesulfonic acid sodium salt. The target molecular structure and synthesis route were presented in Scheme 1.

Materials and Instrumentation

All commercially available starting materials, reagents, and solvents were used as supplied and were obtained from TCI, Acros, and Chengdu Changzheng. Nafion®117 membrane was obtained from DuPont.

^{1}H-Nuclear magnetic resonance (^{1}H-NMR) spectrum was measured by using a Bruker AV II-600 spectrometer. DSC measurement was performed by a TA-modulated Netzsch DSC 204 F1. Thermogravimetric analysis (TGA) was carried out by a TA instrument Netzsch TGA 209C. The scanning of DSC and TGA was both with a rate of 10°C min^{-1} heating/cooling under a nitrogen atmosphere. FTIR spectrum was recorded using a NEXUS 670 FTIR spectrometer. The polarizing micrographs were captured by using a Weitu XPL-30TF equipped with a WT-3000 hot stage. The pH value was determined by using a Youke PHS-3C acidometer. X-ray diffraction (XRD) data were collected on a Philips X'Pert Pro diffractometer using Cu Kα radiation at 40 kV and 40 mA. The molecular weight of the polymer was determined by a high-temperature gel permeation chromatography systems with PL 220 using 1,2,4-trichlorobenzene as an eluent. Elemental analysis was done by using a Euro EA3000 CHNS/O Elemental Analyzer. EIS was recorded on an electrochemical workstation consisting of an EG&G Princeton Applied Research potentiostat/galvanostat model 273A and PAR lock-in-amplifier model 5210 connected to a PC running electrochemical impedance software (frequency range: 10 mHz to 100 kHz; applied voltage: 10 mV). Scanning electron microscopy measurements were performed on a JEOL JSM-6510LV at an accelerating voltage of 20 kV.

Synthesis of the Sulfonated Poly(methyl acrylate)

All reactions were carried out using a dry nitrogen atmosphere. 4-(6-Bromohexoxy)−4′-hydroxy biphenyl (**1**) and 4-(6-acryloyloxyhexyloxy)benzoyl chloride (**2**) were synthesized according to the procedures described previously.[19,20] The brominated mesomorphic poly(methyl acrylate) ($\mathbf{P_{Br}}$) was prepared according to our previous report.[18]

2-Hydroxyethanesulfonic acid sodium salt (0.28 g, 1.93 mmol) and sodium hydride (0.05 g, 2.08 mmol) were added into a flask containing *N*-methyl-2-pyrrolidone (5 mL). After stirring for 30 min, $\mathbf{P_{Br}}$ (1 g, 1.61 mmol) was added into the solution. The mixture was stirred at room temperature for 4 days and then acidified by hydrochloric acid (1 mol L^{-1}). After that, the mixture was poured into methanol, and the precipitate was washed with water and ethyl acetate in turns. A white solid of sulfonated poly(methyl acrylate) ($\mathbf{P_{S45}}$; 0.97 g) was obtained. The presence of sulfonic moieties in $\mathbf{P_{S45}}$ was confirmed by the ^{1}H-NMR and FTIR spectra, as shown in Figures 1 and 2. ^{1}H-NMR (600 MHz $CDCl_3$, 55°C): 8.13, 7.51, 7.29, 6.95 (m, 12H; Ar-H), 4.05 (m, 6.9H; CH_2—OOC, CH_2—O), 3.67 (t, 0.9H;

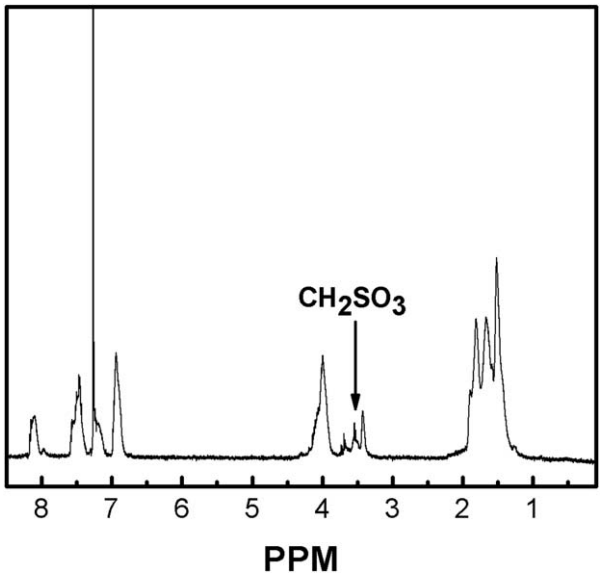

Figure 1. ^{1}H-NMR spectrum of $\mathbf{P_{S45}}$ in $CDCl_3$ at 55°C.

CH_2—O), 3.54 (t, 0.9H; CH_2SO_3), 3.40 (m, 1.1H; CH_2Br), 1.75–1.24 (m, 18H; CH_2). FTIR (KBr): $v = 931$, 2856, 1732 (C═O), 1640, 1498, 1471, 1393, 1288 (Ar-O—C), 1165, 1070 (C—O—C), 1032 (O═S═O), 997, 825 (S—O), 803, 557 (C—Br) cm^{-1}. $M_w = 1 \times 10^4$ g mol^{-1}, $M_w/M_n = 1.67$. Anal. found: C, 65.21; H, 6.82; S, 2.19. The degree of sulfonation determined by the elemental analysis was 0.45.

RESULTS AND DISCUSSION

Mesophases of $\mathbf{P_{S45}}$

The TGA curve of $\mathbf{P_{S45}}$ measured over the temperature range from 50 to 400°C is shown in Figure 3. The thermal decomposition temperature corresponding to 5% mass loss was 299°C. We annealed $\mathbf{P_{S45}}$ in the isotropic state (at 230°C) for 1 h and examined the annealed sample by DSC. The DSC curve (Figure 4) suggested that a glass transition (at 102°C) and two-phase transitions

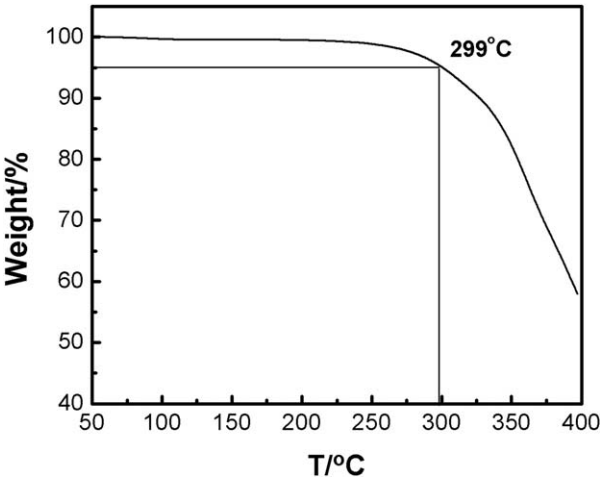

Figure 3. TGA curve of $\mathbf{P_{S45}}$.

happened during the heating scan. The phase transitions were assigned based on POM observation. When $\mathbf{P_{S45}}$ was heated to 147°C, a nonspecific birefringent texture [Figure 5(a)] was observed, and an undefined mesophase (**M**) was assigned tentatively. On further heating to 191°C, a characteristic marble texture [Figure 5(b)] for the nematic phase was developed. The birefringence disappeared as $\mathbf{P_{S45}}$ became isotropic at 227°C. During the cooling scan, only one distinct exothermic transition was observed at 220°C. According to the POM observation, only exothermic peak corresponded to the isotropic–nematic transition. There was no transition peak corresponding to the crystallization. It was expected that the crystallization process was extremely slow.

The liquid-crystal phase assignment has also been performed based on the temperature-dependent XRD measurement. Only a very weak reflection was observed at $2\theta = 21°$ (4.2 Å) in the XRD pattern obtained for $\mathbf{P_{S45}}$ in the **M** phase [Figure 6(a)]. Lateral spacing of orientated mesogens in partially molten side chains was assumed to account for the reflection. The XRD pattern for $\mathbf{P_{S45}}$ collected at 210°C [Figure 6(b)] showed a typical

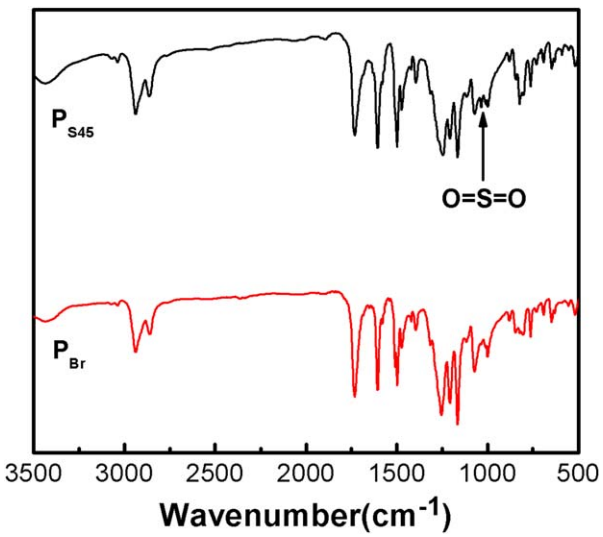

Figure 2. FTIR spectra of $\mathbf{P_{S45}}$ and $\mathbf{P_{Br}}$. [Color figure can be viewed in the online issue, which is available at wileyonlinelibrary.com.]

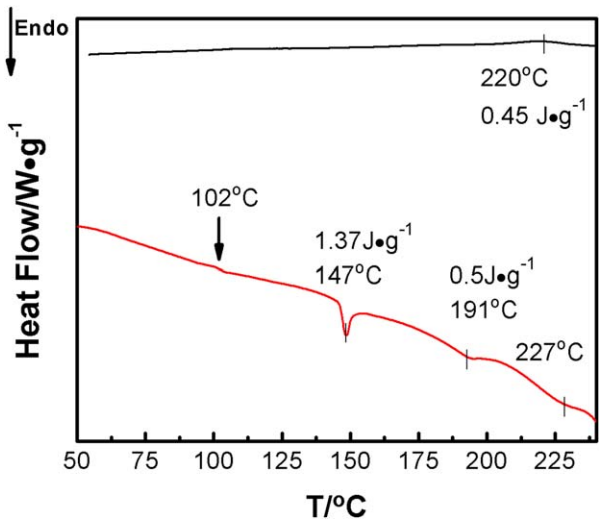

Figure 4. DSC thermograms of $\mathbf{P_{S45}}$. [Color figure can be viewed in the online issue, which is available at wileyonlinelibrary.com.]

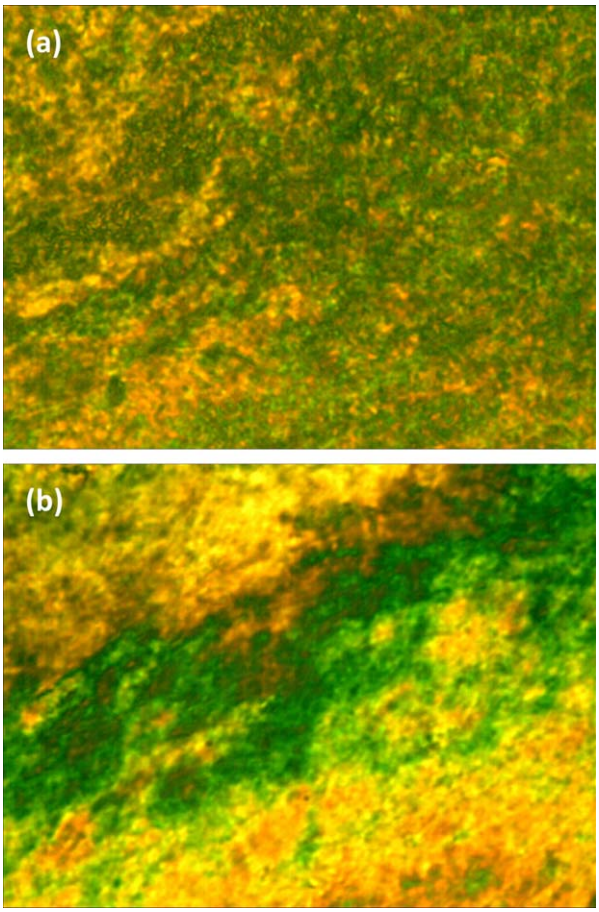

Figure 5. Polarized optical micrographs of $\mathbf{P_{S45}}$ at 170°C (a) and 210°C (b) during the heating scan (×600). [Color figure can be viewed in the online issue, which is available at wileyonlinelibrary.com.]

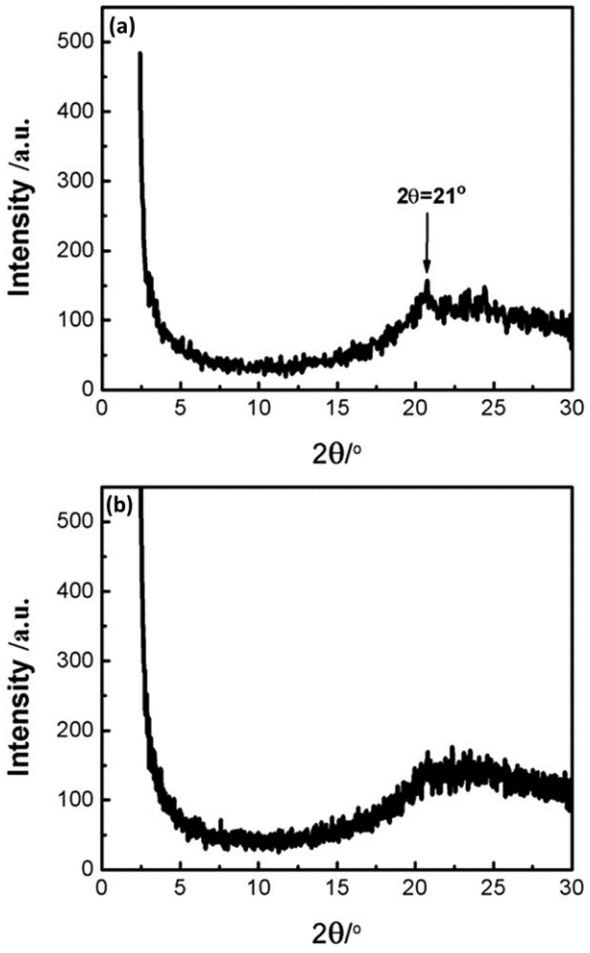

Figure 6. XRD patterns of $\mathbf{P_{S45}}$ at 170°C (a) and 210°C (b).

nematic characteristic of broad peak at around $2\theta = 20°–25°$, classically due to average intermolecular spacings of approximately 3–5 Å in the nematic phase, and no peak appeared in the small angle region.

POM observation suggested that $\mathbf{P_{S45}}$ preserved its original morphology when it was quenched using liquid nitrogen from the nematic phase. In contrast with the sample resulted from the smectic phase,[18] the quenched nematic $\mathbf{P_{S45}}$ did not form uniformly patterned structures on a macroscopic scale even after shearing (Figure 7).

Electrochemical Properties of $\mathbf{P_{S45}}$

Ion-exchange capacity (IEC, mmol of exchangeable H^+ ions per unit mass) of $\mathbf{P_{S45}}$ was examined by acid–base titration as follows. The sample dried to a constant weight was soaked in a 0.1 mol L^{-1} NaCl solution for 24 h to liberate the sulfonic acid protons. The released protons were titrated against a 0.01 mol L^{-1} standardized NaOH solution using a phenolphthalein indicator and an acidometer. The corresponding IEC value was calculated using the following equation:

$$\mathrm{IEC} = C_{H^+} V_{\mathrm{sol}} / W_{\mathrm{dry}}, \quad (1)$$

where C_{H^+}, V_{sol}, and W_{dry} represented the concentration of H^+ ions (mmol cm^{-3} ≅ mequiv cm^{-3}), the volume of extraction solution (cm^3), and the weight of the dried sample (g). The experimental IEC of $\mathbf{P_{S45}}$ was determined to be 0.72 mequiv g^{-1}, which was lower than that of Nafion®117 membrane (0.91 mequiv g^{-1}).[21] There was a small difference (2.8%) between sulfonation degrees determined by acid–base titration and elemental analysis.

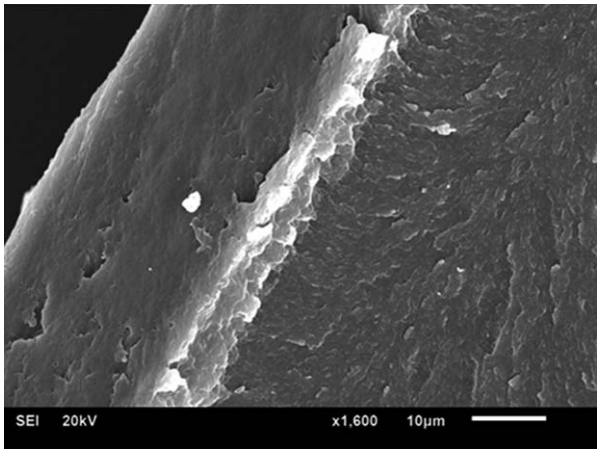

Figure 7. Scanning electron microscopic micrograph of the quenched nematic $\mathbf{P_{S45}}$.

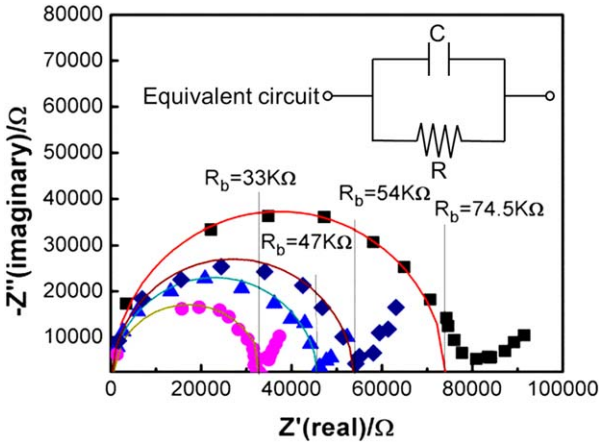

Figure 8. Impedance spectroscopies of $\mathbf{P}_{S45}$ at 180°C (■), 190°C (◆), 200°C (▲), and 210°C (●). [Color figure can be viewed in the online issue, which is available at wileyonlinelibrary.com.]

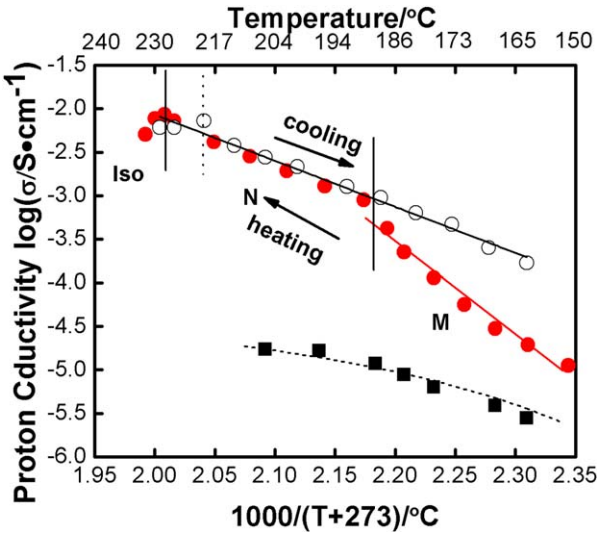

Figure 9. Anhydrous proton conductivities as a function of temperature for $\mathbf{P}_{S45}$ during heating (●), $\mathbf{P}_{S45}$ during cooling (○), and Nafion®117 membrane during heating (■) (—, Arrhenius fitting; ----, Vogel-Tamman-Fulcher fitting). [Color figure can be viewed in the online issue, which is available at wileyonlinelibrary.com.]

$\mathbf{P}_{S45}$ was dried under vacuum overnight before electrochemical characterization. The unaligned sample was sandwiched between two indium tin oxide glass slides and measured in the form of film by the previously reported EIS technique.[22] Thickness d and area A of the film were 0.014 cm and 0.08 cm^2, respectively. Impedance spectra for $\mathbf{P}_{S45}$ were recorded during the heating and cooling scans. Impedance responses at temperatures higher than 165°C were characterized by the semicircles at high frequencies, as shown in Figure 8. The impedance spectrum can be ideally modeled as a parallel RC circuit (R: resistor, C: capacitor) and divided into imaginary (Z'') and real (Z') components. The resistance (R_b) was estimated from the intersection of the real axis (Z') and the semicircle of the impedance spectrum. The proton conductivity σ can be calculated using the following equation:

$$\sigma = d/(R_b A). \quad (2)$$

$\mathbf{P}_{S45}$ did not exhibit electronic conductivity under direct current electric fields and diffusible proton carriers like water molecules did not exist. Therefore, the conductivities of $\mathbf{P}_{S45}$ were purely due to anhydrous proton conduction. Proton conductivities at temperatures from room temperature to the isotropic state are summarized in Table I. When $\mathbf{P}_{S45}$ was heated to the mesophase state (>150°C), an abrupt increase in conductivity from 10^{-7} to 10^{-5} S cm^{-1} was observed. Similar phenomenon was also found for liquid crystal poly(azomethine)s exhibiting semiconductor behavior.[23]

The anhydrous proton conductivities of $\mathbf{P}_{S45}$ in the mesophases measured as a function of temperature are shown in Figure 9. During the heating scan, two segments of Arrhenius profiles [plot of log σ versus $(T+273)^{-1}$ is a straight line] could be discerned in the temperature range of mesophases. The intersection point was found at the vicinity of the **M**-nematic transition. The Arrhenius behavior implied that the proton conduction in $\mathbf{P}_{S45}$ was rather dominated by the Grotthuss mechanism.[24,25] In the unaligned polydomain $\mathbf{P}_{S45}$, sulfonic acid groups from neighboring domains were possibly located close to each other at interfaces to form continuous conduction channels. We proposed that anhydrous proton conduction occurred along the interfaces between polydomains, as schematically illustrated in Figure 10. The estimated Arrhenius activation energies of proton conduction in the **M** phase and the nematic phase during the heating scan were 120 and 95 kJ mol^{-1}, respectively. It was speculated that higher fluidity in the nematic phase lowered the energy required for proton hopping between neighboring sulfonated sites. The conductivity reached the maximum value of 10^{-2} S cm^{-1} at 227°C and decreased right after the nematic–isotropic transition. Both temperature and fluidity in the isotropic phase were higher than those in the nematic phase.[26] The decreased conductivities in the isotropic phase suggested that the nematic order favored the anhydrous proton conduction in $\mathbf{P}_{S45}$. During the cooling scan, conductivities began to decrease at the isotropic–nematic transition (220°C) and followed the Arrhenius law with constant activation energy (95 kJ mol^{-1}). The thermal

Table I. Proton Conductivities of $\mathbf{P}_{S45}$ at Temperatures from Room Temperature to the Isotropic State

T (°C)	σ (S cm^{-1})	T (°C)	σ (S cm^{-1})	T (°C)	σ (S cm^{-1})	T (°C)	σ (S cm^{-1})
30	1.00×10^{-8}	150	1.12×10^{-5}	183	4.21×10^{-4}	215	4.14×10^{-3}
50	1.30×10^{-8}	165	1.85×10^{-5}	187	8.92×10^{-4}	223	7.25×10^{-3}
80	3.60×10^{-8}	170	5.63×10^{-5}	194	1.29×10^{-3}	227	8.59×10^{-3}
110	1.60×10^{-7}	175	1.14×10^{-4}	201	1.93×10^{-3}	230	7.73×10^{-3}
140	6.50×10^{-7}	180	2.25×10^{-4}	208	2.83×10^{-3}	233	5.04×10^{-3}

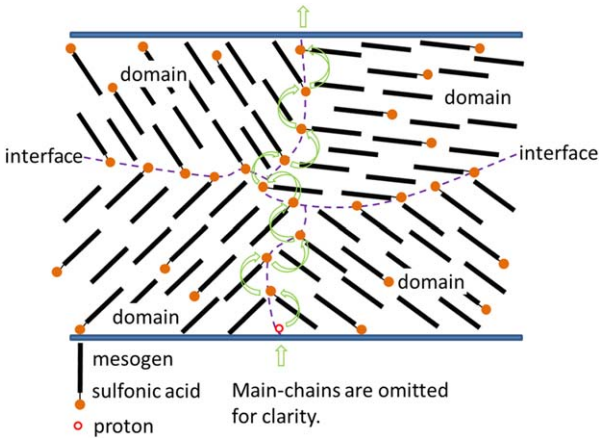

Figure 10. Schematic illustration of proton-conducting channels in the nematic $\mathbf{P_{S45}}$. [Color figure can be viewed in the online issue, which is available at wileyonlinelibrary.com.]

history dependence of proton conductivities was consistent with the phase transitions revealed by the DSC traces.

Conductivities of the nonmesomorphic Nafion®117 membrane with an equivalent IEC (0.91 mequiv g^{-1}) were also evaluated under the anhydrous conditions to discuss the effect of the nematic liquid crystal on electrochemical performance. Nafion®117 membrane exhibited essentially identical proton conduction behavior during the heating and cooling scans. The temperature dependence of the conductivity of anhydrous Nafion®117 membrane seemed to obey the Vogel-Tamman-Fulcher relationship, which indicated that the conduction was dominated by segmental motion of the polymer.[27–29] The maximum anhydrous proton conductivity of Nafion®117 membrane was observed at about 215°C. It was 2 orders of magnitude lower than that of nematic $\mathbf{P_{S45}}$ at the same temperature. The result suggested that the proton hopping in the nematic $\mathbf{P_{S45}}$ conducted protons more efficiently than the segmental motion in Nafion®117 membrane.

CONCLUSIONS

In this study, $\mathbf{P_{S45}}$ exhibiting the nematic phase at medium temperatures was prepared by postpolymerization functionalization of a mesogenic precursor. Anhydrous proton conductivities of the polymeric electrolyte measured by EIS followed the Arrhenius law, and the estimated activation energy was 95 kJ mol^{-1} in the nematic phase. The conductivities of the nematic electrolyte were 2 orders of magnitude higher than those of anhydrous Nafion®117 membrane. It was speculated that the orientational order and fluidity of the nematic liquid crystal promoted anhydrous proton conduction in the polymeric electrolyte. Composite membranes consisting of the nematic sulfonated poly(methyl acrylate) and supporting substrate are expected to be applicable in medium-temperature fuel cells.

ACKNOWLEDGMENTS

This work was supported by the National Natural Science Foundation of China under the Grant No. 20974068.

REFERENCES

1. Kreuer, K. D. *Chem. Mater.* **1996**, *8*, 610.
2. Costamagna, P.; Srinivansan, S. *J. Power Sources* **2001**, *102*, 242.
3. Choi, P.; Jalani, N. H.; Datta, R. *J. Electrochem. Soc.* **2005**, *152*, E123.
4. Seeliger, D.; Hartnig, C.; Spohr, E. *Electrochim. Acta* **2005**, *50*, 4234.
5. Bose, S.; Kuila, T.; Nguyen, T. X. H.; Kim, N. H.; Lau, K.; Lee, J. H. *Prog. Polym. Sci.* **2011**, *36*, 813.
6. Li, Q.; He, R.; Gao, J.; Jensen, J. O.; Bjerrum, N. J. *J. Electrochem. Soc.* **2003**, *150*, A1599.
7. Alberti, G.; Casciola, M.; Massinelli, L.; Bauer, B. *J. Membr. Sci.* **2001**, *185*, 73.
8. Shao, Z.; Joghee, P.; Hsing, I. *J. Membr. Sci.* **2004**, *229*, 43.
9. Yang, C.; Costamagna, P.; Srinivasan, S.; Benziger, J.; Bocarsly, A. B. *J. Power Sources* **2001**, *103*, 1.
10. Yamada, M.; Honma, I. *Polymer* **2005**, *46*, 2986.
11. Xiao, L.; Zhang, H.; Scanlon, E.; Ramanathan, L. S.; Choe, E. W.; Rogers, D.; Apple, T.; Benicewicz, B. C. *Chem. Mater.* **2005**, *17*, 5328.
12. Carbone, A.; Pedicini, R.; Saccà, A.; Gatto, I.; Passalacqua, E. *J. Power Sources* **2008**, *178*, 661.
13. Lobato, J.; Cañizares, P.; Rodrigo, M. A.; Linares J. *J. Electrochim. Acta* **2007**, *52*, 3910.
14. Schadt, M. *Annu. Rev. Mater. Sci.* **1997**, *27*, 305.
15. Huang, Y.; Cong, Y.; Li, J.; Wang, D.; Zhang, J.; Xu, L.; Li, W.; Li, L.; Pan, G.; Yang, C. *Chem. Commun.* **2009**, 7560.
16. Ueda, S.; Kagimoto, J.; Ichikawa, T.; Kato, T.; Ohno, H. *Adv. Mater.* **2011**, *23*, 3071.
17. Chow, C.-F.; Roy, V. A. L.; Ye, Z.; Lam, M. H. W.; Lee, C. S.; Lau, K. C. J. *J. Mater. Chem.* **2010**, *20*, 6245.
18. Tan, S.; Wang, C.; Wu, Y. *J. Mater. Chem. A* **2013**, *1*, 1022.
19. Millaruelo, M.; Oriol, L.; Serrano, J. L.; Piñol, M.; Sáez, P. L. *Mol. Cryst. Liq. Cryst.* **2004**, *411*, 451.
20. Kuo, T.; O'Brien, D. F. *Langmuir* **1991**, *7*, 584.
21. Hickner, M. A.; Pivovar, B. S. *Fuel Cells* **2005**, *5*, 213.
22. Yoshio, M.; Mukai, T.; Kanie, K.; Yoshizawa, M.; Ohno, H.; Kato, T. *Adv. Mater.* **2002**, *14*, 351.
23. Iwan, A.; Palewicz, M.; Sikora, A.; Chmielowiec, J.; Hreniak, A.; Pasciak, G.; Bilski, P. *Synth. Met.* **2010**, *160*, 1856.
24. Armand, M. *Solid State Ionics* **1983**, *9*, 745.
25. Bouchet, R.; Siebert, E. *Solid State Ionics* **1999**, *118*, 287.
26. Singh, S. *Phys. Rep.* **2000**, *324*, 107.
27. Kuo, C.; Li, W.; Chen, P.; Liao, J.; Tseng, C.; Wu, T. *Int. J. Electrochem. Sci.* **2013**, *8*, 5007.
28. Noto, V. D.; Piga, M.; Giffin, G. A.; Quartarone, E.; Righetti, P.; Mustarelli, P.; Magistris, A. *Phys. Chem. Chem. Phys.* **2011**, *13*, 12146.
29. Pu, H.; Liu, Q.; Liu, G. *J. Membr. Sci.* **2004**, *241*, 169.